

## Sensitivity And Stability Analyses Of A Lassa Fever Disease Model With Control Strategies

Mary Oluwabunmi AKINADE<sup>1</sup>, Ayodeji Sunday AFOLABI<sup>2</sup>

<sup>1</sup> Department of Computational Mathematics, Pan African University  
Institute for Basic Sciences, Technology and Innovation (PAUSTI),  
P.O. Box 62000-00200, Nairobi-Kenya

<sup>2</sup> Department of Mathematical Sciences, The Federal University of Technology Akure,  
P.M.B. 704, Akure, Ondo State, Nigeria

---

### Abstract

**Background:** Lassa fever disease is a fatal zoonotic hemorrhagic disease caused by Lassa virus and endemic in West African countries. The aim of this paper is the application of mathematical modeling and analyses in controlling the spread of this disease.

**Materials and Methods:** In this paper, a mathematical model which represents the transmission and control processes of Lassa fever disease among human and vector hosts is developed. The model is developed as a coupled system of 7 ordinary differential equations using the compartmental disease modeling approach. Three control strategies are incorporated into the model and the model analyzed for the existence of a positively invariant region within which its solutions are uniformly bounded. The model equations are solved numerically using the MATLAB ode45 method and simulations performed to visualize the effects of each control parameter on the spread and control of the disease. Furthermore, local and global stability analyses of the model's equilibrium point are performed using the next-generation matrix approach and the direct Lyapunov method respectively with sensitivity analyses carried out on the model parameters.

**Results:** The stability analyses performed on the disease-free equilibrium state of the model indicate that the disease will not invade the studied population but can be controlled if the parameters of the model are implemented in such population. The sensitivity analyses results show the sensitiveness of each model parameter to the transmission of the disease. The numerical simulation of the model suggests that the availability of the three control strategies in an endemic area results in the eradication of the disease over time.

**Conclusion:** It is concluded that the developed model is viable to represent the real-life situation being modeled, hence, it is recommended that the model and its results be implemented in an endemic area.

**Keywords:** Lassa Fever, Mathematical Model, Numerical Simulation, Sensitivity Analyses, Stability Analyses

---

Date of Submission: 26-12-2019

Date of Acceptance: 11-01-2020

---

### I. Introduction

The greatest threat to human existence, apart from environmental hazards such as fire outbreaks and earthquakes, are infectious diseases, one of which is the deadly Lassa fever disease. Infectious diseases are caused by pathogenic micro-organisms, such as bacteria, viruses, parasites or fungi, and can spread directly or indirectly from one person to another (CDC, 2018).

Lassa fever (LF) is an acute hemorrhagic viral disease caused by the Lassa virus (LASV) and predominantly spreading in West African countries. The major host of the LASV is the Autochthonous *Mastomys natalensis* rat specie. The mode of transmission of the LF disease is via contact with the bodily fluids and secretions of an infected person or animal. Lassa virus has an incubation period of about 6 to 21 days in human host, a period in which such an infected person do not exhibit any noticeable symptom of the infection. The fatality rate of the Lassa fever in symptomatic patients who are receiving treatment is between 15% and 20%. A total of 80% of humans infected with the LF disease are without symptoms, although they are infectious (Du-Toit, 2018). According to the world health organization, there are about 300,000 to 500,000 cases of Lassa fever disease across West Africa which result in about 5,000 deaths per year (WHO, 2018).

Onuorah et al. (2016a) developed a mathematical model for the spread of Lassa fever. The disease free equilibrium (DFE) was analyzed for its existence and stability. The results of this analysis showed that if the basic reproduction number,  $R_0$ , is less than or equal to 1, and there do not exist an endemic equilibrium point (EEP) for the disease, then the disease will die out, otherwise the disease will persist in the population. James and Akinyemi (2015) performed the stability analysis of LF transmission, but with the assumption of the existence of quarantine for the infected human population and permanent immunity for the recovered human population. The results of

this investigation was that the disease can be easily controlled if these assumptions can be implemented into all LF endemic populations. This result was in agreement with the analysis of Bawa et al. (2013) in which the model that represented the Lassa fever disease incorporated standard incidence rate and it was assumed that this rate can be predetermined.

Eze et al. (2010) analyzed and discussed the impact of Lassa fever in some endemic areas including the northern part of Edo State in Nigeria with high rate of infection on contact persons. According to this research, each year at least 32.26% (4,096) of patients with febrile illness that come to Irua specialist teaching hospital (ISTH) in Edo state has Lassa fever. This figure was said to be more than that of malaria, tuberculosis or HIV/AIDS. Adewale et al. (2016) developed a mathematical model for the transmission of Lassa fever with isolation of infected individuals and obtained the basic reproduction number,  $R_0$ . The analysis of the model showed that the DFE is locally and globally asymptotically stable, with the threshold quantity,  $R_0$ , less than 1. It was also concluded that an EEP, a positive steady state solution for which the disease persists in the studied population, may exist for the developed model under certain conditions.

Onuorah et al. (2016b) developed a mathematical model for the transmission of LF. The basic reproduction number which can be used to control the transmission dynamics of the disease was obtained and the conditions for local and global stabilities of the DFE was established. It was concluded that though the DFE is globally asymptotically stable (with  $R_0 < 1$ ), the disease will still continue to spread due to the unavailability of controls. Omale & Edibo (2017) modeled the transmission of Lassa fever virus between humans and rodents with control strategies as a six-dimensional ordinary differential equation. Stability analysis of the DFE was performed and the basic reproduction number obtained using the next generation operator approach. The existence of endemic equilibrium was further determined. The study, then, concluded that more awareness should be conducted in the affected areas so as to prevent more outbreaks of the disease.

Subsequently, Obabiyi and Onifade (2017) developed a new mathematical model for LF disease. The maximum principle theorem was used to establish the positivity and the boundedness results of the model's solutions. Conditions were derived for the existence of disease free and endemic equilibrium points, and stabilities analyzed. The study concluded that a threshold parameter,  $R_0$ , exists and the disease can persist if and only if  $R_0$  exceeds 1. The study further suggested that maintaining hygienic environment, use of new needle when taking injection and control of the rodent carrying the virus are effective strategies against the spread of the disease.

Akinade et al. (2019) developed a mathematical model to represent the transmission processes of the LF disease in human and vector hosts. This model was used to incorporate the carrier human population, which caters for the asymptomatic patients, into the Lassa fever pandemic. The basic reproduction number obtained, 0.46252994, coupled with the existence of an EEP for the model suggests that even though the disease may not invade the studied population, it may however persist in it. This research recommended that necessary control parameters, including the early diagnosis of the non symptomatic patients, be introduced in a Lassa fever model and analyzed for their significance on the spread and control of the disease.

Despite the attempts by several researchers to combat the spread of the deadly Lassa fever disease, the disease still continues to spread and in fact at an increasing fatal rate. In this paper, we extended the work of Akinade et al. (2019) by incorporating three control parameters into the developed model. We also perform the sensitivity analyses of the model's parameters, including the controls, in order to measure their individual sensitivity index to the spread and control of the disease. Furthermore, we perform the numerical simulation of the developed control model in order to visualize the state solution of the developed model over time.

## II. Materials and Methods

The method employed in developing the Lassa fever control model in this study is the compartmental disease modeling approach. In this new Lassa fever model, there are 7 state variables to indicate the various mutually exclusive human and vector populations as shown in Table 1 below. Similarly, there are 20 parameters which describe the transmission and control processes of the Lassa fever infection in human and vector hosts, as further described.

The rate at which humans migrate into a Lassa fever endemic population so that they become susceptible to the infection is denoted by  $\alpha_h$  while that of the vector is denoted by  $\alpha_v$ . Similarly,  $\mu_h$  and  $\mu_v$  represent respectively the rate at which humans and vector die naturally. Meanwhile  $\delta_h$  and  $\delta_v$  represent the disease induced death rate for human and vector populations respectively.

**Table 1:** The Model State Variables

Variables	Description
$S_h(t)$	Susceptible Human Population
$C_h(t)$	Carrier Human Population
$I_h(t)$	Infected Human Population
$T_h(t)$	Treated Human Population

$R_h(t)$	Recovered Human Population
$S_v(t)$	Susceptible Vector Population
$I_v(t)$	Infected Vector Population

Furthermore, parameters  $\beta_h$  and  $\beta_v$  represent the rate at which humans contract the LF infection via contacts with another infected humans and via contact with an infected vector respectively. Similarly,  $\omega_v$  represents the rate at which the vectors become infected with the disease. For the developed model, treatment is given to the infected vector population at the rate  $\gamma_2$  while the efficacy of this treatment is denoted by  $\beta$ . The recovery rate of the treated human population from the infection is denoted by  $\gamma_3$  while the recovery rate of the infected human population from the infection by their own natural immunity is denoted by  $\gamma_4$ . In addition, the recovered human population loses their immunity against the disease and become susceptible again at the rate  $\omega_h$ .

In order to cater for the transmission and recovery processes of the newly incorporated carrier human population, new model parameters which were not in existence in previous literature were incorporated into the model. These parameters are the contracting rate of the infection for susceptible human population via interaction with the carrier human population denoted by  $\beta_c$ , the rate of progression from the carrier human population to the infected human population denoted by  $\sigma_h$  and the rate of recovery of the carrier human population by natural immunity denoted by  $\gamma_1$ .

Lastly, the control strategies in the model are; early diagnosis (and treatment of the carriers) which results in their migration into the carrier human population, vaccination of the susceptible human population which leads to their migration into the recovered human population and the use of Rodenticide on the vector populations, efficacy of which leads to their death. These controls are denoted by  $u_1$ ,  $u_2$  and  $u_3$  respectively. Figure 1 below represents the schematic flow diagram of the Lassa fever control model. The following are the assumptions made in the development of the model:

1. The human-carriers are diagnosed and begin treatment before onset of symptoms.
2. Vaccinated humans are considered to have recovered from the infection.
3. The effect of the Rodenticide use is the death of the vectors, susceptible and infected alike.

**The Lassa Fever Control Model**

$$\frac{dS_h}{dt} = \alpha_h + \omega_h R_h - (u_1 \beta_c C_h + \beta_h I_h + u_3 \beta_v I_v) S_h - u_2 S_h - \mu_h S_h \quad (2.1)$$

$$\frac{dC_h}{dt} = (u_1 \beta_c C_h + \beta_h I_h + u_3 \beta_v I_v) S_h - (u_1 \sigma_h + \gamma_1 + u_1 \delta_h + u_1 + \mu_h) C_h \quad (2.2)$$

$$\frac{dI_h}{dt} = u_1 \sigma_h C_h - \gamma_2 I_h - \gamma_4 I_h - \delta_h I_h - \mu_h I_h \quad (2.3)$$

$$\frac{dT_h}{dt} = u_1 C_h + \gamma_2 I_h - \beta \gamma_3 T_h - (1 - \beta) \delta_h T_h - \mu_h T_h \quad (2.4)$$

$$\frac{dR_h}{dt} = u_2 S_h + \gamma_1 C_h + \gamma_4 I_h + \beta \gamma_3 T_h - \omega_h R_h - \mu_h R_h \quad (2.5)$$

$$\frac{dS_v}{dt} = \alpha_v - \omega_v S_v - u_3 S_v - \mu_v S_v \quad (2.6)$$

$$\frac{dI_v}{dt} = \omega_v S_v - \delta_v I_v - u_3 I_v - \mu_v I_v \quad (2.7)$$

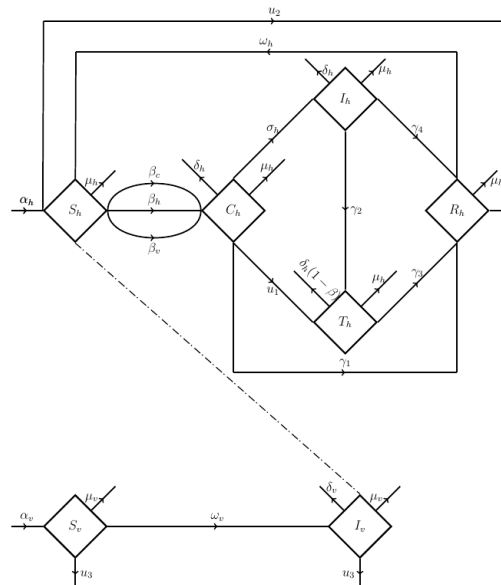


**Figure 1: Schematic Flow Diagram of the Lassa Fever Control Model**

### III. Results

In this section, we present the three major analyses performed on the Lassa fever control model.

#### 3.1 The Invariant Region of the Control Model

In order to justify that the model is epidemiologically visible, that is the model and its predictions make epidemiological sense, we present the basic qualitative property of the model. This involves finding the set within which the model can be sufficiently studied (i.e., the invariant region of the model). For the model, the total human population is denoted as  $N_h(t)$  while that of the vector population is denoted by  $N_v(t)$ .

Thus  $N_h(t) = S_h(t) + C_h(t) + I_h(t) + T_h(t) + R_h(t)$  and  $N_v(t) = S_v(t) + I_v(t)$ .

From equations 2.1 to 2.7;

$$\frac{dN_h}{dt} = \alpha_h - \mu_h N_h - u_1 \delta_h C_h - \delta_h I_h - (1 - \beta) \delta_h T_h$$

$$\frac{dN_h}{dt} \leq \alpha_h - \mu_h N_h \quad (3.1)$$

Similarly;

$$\frac{dN_v}{dt} = \alpha_v - \mu_v N_v - \delta_v I_v - u_3 N_v$$

$$\leq \alpha_v - \mu_v N_v \quad (3.2)$$

By integrating both sides of (3.1), we have;

$$\int \frac{dN_h}{\alpha_h - \mu_h N_h} \leq \int dt$$

Thus,

$$\ln(\alpha_h - \mu_h N_h) \geq -(\mu_h t + C)$$

$$(\alpha_h - \mu_h N_h) \geq Ae^{-\mu_h t}$$

where C and A are constants of integration.

Let  $N_h(0) = N_0 \geq 0$ , then;

$$(\alpha_h - \mu_h N_0) \geq A$$

Accordingly,

$$(\alpha_h - \mu_h N_h) \geq (\alpha_h - \mu_h N_0)e^{-\mu_h t}$$

$$N_h(t) \leq \frac{\alpha_h}{\mu_h} - \frac{(\alpha_h - \mu_h N_0)}{\mu_h} e^{-\mu_h t}$$

$$N_h(t) \rightarrow \frac{\alpha_h}{\mu_h} \text{ as } t \rightarrow \infty$$

Thus,  $N_h(t) \in [0, \frac{\alpha_h}{\mu_h}]$ .

Similarly, by solving (3.2), we obtain;

$$N_v(t) \in [0, \frac{\alpha_v}{\mu_v}].$$

Hence, the region in which the solution to the model is bounded is:

$$\Omega = \{(S_h, C_h, I_h, T_h, R_h) \in R_+^5 \cup (S_v, I_v) \in R_+^2: N_h(t) \leq \frac{\alpha_h}{\mu_h}, N_v(t) \leq \frac{\alpha_v}{\mu_v}\} \quad (3.3)$$

We therefore conclude that the region within which the solution to the model's equations are contained is positively invariant and hence the model is epidemiologically and mathematically well-posed.

#### 3.2 Stability Analysis of the Model

In this section, we obtain the disease free equilibrium point of the model and test for its local and global asymptotic stabilities. A DFE point is a state solution to the model in which the studied population remains in the absence of the disease. In this solution, all state variables except the susceptible populations are equated to zero.

The DFE of the model is defined as  $(S_h^*(t), 0, 0, 0, 0, S_v^*(t), 0)$  satisfying  $\frac{dS_h}{dt} = \frac{dC_h}{dt} = \frac{dI_h}{dt} = \frac{dT_h}{dt} = \frac{dR_h}{dt} = 0$  and

$$\frac{dS_v}{dt} = \frac{dI_v}{dt} = 0$$

By equating equations (2.1) to (2.7) to 0 and substituting  $C_h = I_h = T_h = R_h = I_v = 0$ ,

$$\text{We obtain } S_h^* = \frac{\alpha_h}{(u_2 + \mu_h)} \text{ and } S_v^* = \frac{\alpha_v}{(u_3 + \mu_v)}.$$

Accordingly, the DFE is obtained as:

$$E_0 = (\frac{\alpha_h}{(u_2 + \mu_h)}, 0, 0, 0, 0, \frac{\alpha_v}{(u_3 + \mu_v)}, 0) \quad (3.4)$$

**3.2.1 Local Asymptotic Stability Analysis of the DFE**

Here, we employ the principle of next generation matrix as described by Castillo and Song (2004). This principle states that, the disease free equilibrium point of an infectious disease model is locally asymptotically stable if the basic reproduction number,  $R_0$ , is less than one.

**The Basic Reproduction Number**

According to the principle of next generation matrix, the basic reproduction number is the spectral radius of the next generation matrix  $FV^{-1}$  of the system (2.1) to (2.7).

We define:  $f_i - v_i = \begin{pmatrix} C_h' \\ I_h' \\ T_h' \end{pmatrix}$

$$= \begin{pmatrix} (u_1\beta_c C_h + \beta_h I_h + u_3\beta_v I_v)S_h - (u_1\sigma_h + \gamma_1 + u_1\delta_h + u_1 + \mu_h)C_h \\ u_1\sigma_h C_h - (\gamma_2 + \gamma_4 + \delta_h + \mu_h)I_h \\ u_1 C_h + \gamma_2 I_h - (\beta\gamma_3 + (1 - \beta)\delta_h + \mu_h)T_h \end{pmatrix} \quad (3.5)$$

Accordingly;

$$f_i = \begin{pmatrix} (u_1\beta_c C_h + \beta_h I_h + u_3\beta_v I_v)S_h \\ 0 \\ 0 \end{pmatrix} \quad (3.6)$$

$$v_i = \begin{pmatrix} (u_1\sigma_h + \gamma_1 + u_1\delta_h + u_1 + \mu_h)C_h \\ (\gamma_2 + \gamma_4 + \delta_h + \mu_h)I_h - u_1\sigma_h C_h \\ (\beta\gamma_3 + (1 - \beta)\delta_h + \mu_h)T_h - u_1 C_h - \gamma_2 I_h \end{pmatrix} \quad (3.7)$$

Here,  $f_i$  is defined as the rate of appearance of new infection(s) in compartment  $i$  and  $v_i$  denotes the rate of transfer of individuals into compartment  $i$ , with  $i \in [1,3]$ .

The matrix  $F$  and  $V$  are defined as;

$$F = \begin{pmatrix} \frac{\partial f_1}{\partial C_h} & \frac{\partial f_1}{\partial I_h} & \frac{\partial f_1}{\partial T_h} \\ \frac{\partial f_2}{\partial C_h} & \frac{\partial f_2}{\partial I_h} & \frac{\partial f_2}{\partial T_h} \\ \frac{\partial f_3}{\partial C_h} & \frac{\partial f_3}{\partial I_h} & \frac{\partial f_3}{\partial T_h} \end{pmatrix}$$

$$= \begin{pmatrix} u_1\beta_c S_h & \beta_h S_h & 0 \\ 0 & 0 & 0 \\ 0 & 0 & 0 \end{pmatrix} \quad (3.8)$$

$$V = \begin{pmatrix} \frac{\partial v_1}{\partial C_h} & \frac{\partial v_1}{\partial I_h} & \frac{\partial v_1}{\partial T_h} \\ \frac{\partial v_2}{\partial C_h} & \frac{\partial v_2}{\partial I_h} & \frac{\partial v_2}{\partial T_h} \\ \frac{\partial v_3}{\partial C_h} & \frac{\partial v_3}{\partial I_h} & \frac{\partial v_3}{\partial T_h} \end{pmatrix}$$

$$= \begin{pmatrix} (u_1\sigma_h + \gamma_1 + u_1\delta_h + u_1 + \mu_h) & 0 & 0 \\ -u_1\sigma_h & (\gamma_2 + \gamma_4 + \delta_h + \mu_h) & 0 \\ -u_1 & -\gamma_2 & (\beta\gamma_3 + (1 - \beta)\delta_h + \mu_h) \end{pmatrix} \quad (3.9)$$

Lastly,  $V^{-1} =$

$$\begin{pmatrix} \frac{1}{\delta_h u_1 + \sigma_h u_1 + \gamma_1 + \mu_h + u_1} & 0 & 0 \\ \frac{\sigma_h u_1}{(\delta_h u_1 + \sigma_h u_1 + \gamma_1 + \mu_h + u_1)(\delta_h + \gamma_2 + \gamma_4 + \mu_h)} & \frac{1}{\delta_h + \gamma_2 + \gamma_4 + \mu_h} & 0 \\ \frac{\gamma_2 \sigma_h u_1}{(\delta_h u_1 + \sigma_h u_1 + \gamma_1 + \mu_h + u_1)(\delta_h + \gamma_2 + \gamma_4 + \mu_h)} + \frac{u_1}{\delta_h u_1 + \sigma_h u_1 + \gamma_1 + \mu_h + u_1} & \frac{\gamma_2}{(b\delta_h + \beta\gamma_3 + \mu_h)(\delta_h + \gamma_2 + \gamma_4 + \mu_h)} & \frac{1}{b\delta_h + \beta\gamma_3 + \mu_h} \end{pmatrix}$$

where  $b = (1 - \beta)$ .

Thus, the next generation matrix:

$$G = FV^{-1}$$

$$= \begin{pmatrix} \frac{S_h \beta_c u_1}{\delta_h u_1 + \sigma_h u_1 + \gamma_1 + \mu_h + u_1} + \frac{S_h \beta_h \sigma_h u_1}{(\delta_h u_1 + \sigma_h u_1 + \gamma_1 + \mu_h + u_1)(\delta_h + \gamma_2 + \gamma_4 + \mu_h)} & \frac{S_h \beta_h}{\delta_h + \gamma_2 + \gamma_4 + \mu_h} & 0 \\ 0 & 0 & 0 \\ 0 & 0 & 0 \end{pmatrix} \quad (3.10)$$

The basic reproduction number is computed as the largest eigenvalue of the matrix  $G$  above using the SageMath computational software as:

$$R_0 = \frac{(\beta_c \delta_h + \beta_c \gamma_2 + \beta_c \gamma_4 + \beta_c \mu_h + \beta_h \sigma_h) u_1 S_h^*}{(\delta_h + \gamma_2 + \gamma_4) \gamma_1 + (\delta_h + \gamma_1 + \gamma_2 + \gamma_4) \mu_h + \mu_h^2 + (\delta_h^2 + (\delta_h + 1)(\gamma_2 + \gamma_4 + \mu_h)) + (\delta_h + \gamma_2 + \gamma_4 + \mu_h) \sigma_h + \delta_h) u_1}$$

By substituting the expression for  $S_h^*$  from 3.4, we obtain;

$$R_0 = \frac{(\beta_c \delta_h + \beta_c \gamma_2 + \beta_c \gamma_4 + \beta_c \mu_h + \beta_h \sigma_h) u_1 \alpha_h}{((\delta_h + \gamma_2 + \gamma_4) \gamma_1 + (\delta_h + \gamma_1 + \gamma_2 + \gamma_4) \mu_h + \mu_h^2 + (\delta_h^2 + (\delta_h + 1)(\gamma_2 + \gamma_4 + \mu_h)) + (\delta_h + \gamma_2 + \gamma_4 + \mu_h) \sigma_h + \delta_h) u_1} (u_2 + \mu_h) \tag{3.11}$$

Accordingly, by substituting the values in table (2) below the basic reproduction number;

$$R_0 = 0.0238787 \tag{3.12}$$

The calculated value of  $R_0$  is significantly small and lesser than that obtained by [3] in which the analyzed model do not contain any control strategy. Since the basic reproduction number obtained is less than one, then the DFE is locally asymptotically stable and thus the disease cannot invade the studied population.

**Table 2:** Table of Values for the Model's Parameters

Parameters	Values	Sources
$\alpha_h$	0.080	Estimate
$\mu_h$	0.0000548	Afolabi and Sobowale (2017)
$\omega_h$	0.0085	NCDC (2019)
$\beta_c$	0.000062	Ogabi et al. (2012)
$\beta_h$	0.00012	Estimate
$\beta_v$	0.005	Afolabi and Sobowale (2017)
$\delta_h$	0.01710615	NCDC (2019)
$\mu_v$	0.000167	Estimate
$\sigma_h$	0.10	NCDC (2019)
$\gamma_2$	0.2148541	NCDC (2019)
$\alpha_v$	0.70	Akinpelu and Akinwande (2008)
$\delta_v$	0.05	Estimate
$\omega_v$	0.02	Estimate
$\gamma_3$	0.030	NCDC (2019)
$\gamma_1$	0.0315	Estimate
$\gamma_4$	0.0005	Estimate
$\beta$	0.612	NCDC (2019)
$u_1$	0.0101231	Estimate
$u_2$	0.11231	Estimate
$u_3$	0.050	Estimate

**3.2.2 Global Asymptotic Stability Analysis**

For the global asymptotic stability analysis of the DFE, we employ the method implemented by [6]. The Lassa fever model is denoted by:

$$\begin{cases} \frac{dX}{dt} = F(X, Y) \\ \frac{dY}{dt} = G(X, Y) \end{cases} \tag{3.13}$$

Here,  $X = (S_h, R_h, S_v)$  represents the uninfected population and  $Y = (C_h, I_h, T_h, I_v)$  represents the Infected population. The point  $E_0 = (X^*, 0)$  is said to be globally asymptotically stable if  $R_0 < 1$  and the following two conditions hold:

C1: For  $\frac{dX}{dt} = F(X, 0)$ ,  $E_0$  is globally asymptotically stable.

C2:  $G(X, Y) = AY - G^*(X, Y)$ ,  $G^*(X, Y) \geq 0$  for  $(X, Y) \in \Omega$

**C1:**

$$F(X, 0) = \begin{pmatrix} \alpha_h + \omega_h R_h - (u_2 + \mu_h) S_h \\ u_2 S_h - (\omega_h + \mu_h) R_h \\ \alpha_v - (\omega_v + u_3 + \mu_v) S_v \end{pmatrix} \tag{3.14}$$

The equilibrium solution  $E_0 = (\frac{\alpha_h}{(u_2 + \mu_h)}, 0, 0, 0, 0, \frac{\alpha_v}{(u_3 + \mu_v)}, 0)$  is globally asymptotically stable for  $\frac{dX}{dt} = F(X, 0)$  as shown below:

By solving equation (3.14) using the method of integrating factor, we have:

$$\begin{aligned} \frac{dS_h}{dt} &= \alpha_h + \omega_h R_h - (u_2 + \mu_h) S_h \\ I.F &= e^{\int (u_2 + \mu_h) dt} \\ \frac{d}{dt} (S_h e^{(u_2 + \mu_h)t}) &= (\alpha_h - \omega_h R_h) e^{(u_2 + \mu_h)t} \end{aligned}$$

Thus,  $S_h = \frac{\alpha_h}{(u_2 + \mu_h)} - \frac{1}{e^{(u_2 + \mu_h)t}} \int \omega_h R_h e^{(u_2 + \mu_h)t} dt$

Accordingly,  $S_h(t) \rightarrow \frac{\alpha_h}{(u_2 + \mu_h)}$  as  $t \rightarrow \infty$

Similarly,  $S_v(t) \rightarrow \frac{\alpha_v}{(u_3 + \mu_v)}$  as  $t \rightarrow \infty$

which implies the global convergence of  $E_0$  for  $F(X, 0)$ .

**C2:**

$$G(X, Y) = \begin{pmatrix} (u_1\beta_c C_h + \beta_h I_h + u_3\beta_v I_v)S_h - (u_1\sigma_h + \gamma_1 + u_1\delta_h + u_1 + \mu_h)C_h \\ u_1\sigma_h C_h - (\gamma_2 + \gamma_4 + \delta_h + \mu_h)I_h \\ u_1 C_h + \gamma_2 I_h - (\beta\gamma_3 + b\delta_h + \mu_h)T_h \\ \omega_v S_v - (\delta_v + u_3 + \mu_v)I_v \end{pmatrix} \quad (3.15)$$

$$= AY - G^*(X, Y)$$

Here,

$$A = \begin{pmatrix} -H & 0 & 0 & 0 \\ u_1\sigma_h & -(\gamma_2 + \gamma_4 + \delta_h + \mu_h) & 0 & 0 \\ u_1 & \gamma_2 & -(\beta\gamma_3 + b\delta_h + \mu_h) & 0 \\ 0 & 0 & 0 & -(\delta_v + u_3 + \mu_v) \end{pmatrix}$$

where  $b = (1 - \beta)$  and  $H = (u_1\sigma_h + \gamma_1 + u_1\delta_h + u_1 + \mu_h)$ ;

$$G^*(X, Y) = \begin{bmatrix} -(u_1\beta_c C_h + \beta_h I_h + u_3\beta_v I_v)S_h \\ 0 \\ 0 \\ -\omega_v S_v \end{bmatrix}$$

$$\leq 0$$

Since  $G^*(X, Y) \leq 0$ , then condition 2 is not satisfied. Thus,  $E_0 = (X^*, 0)$  may not be globally asymptotically stable for  $R_0 < 1$ .

### 3.3 Sensitivity Analysis of the Lassa Fever Control Model

As we are interested in controlling the disease within the shortest possible time, we perform the sensitivity analysis of the model's parameters in order to obtain their rate of sensitiveness to the disease transmission and control. This analysis helps us to determine the parameters that have high (or low) impact/significance on the basic reproduction number value. We define the normalized forward sensitivity index of  $R_0$  with respect to a parameter  $p$  as;

$$\begin{aligned} \Gamma_p^{R_0} &= \frac{\partial R_0}{R_0} \div \frac{\partial p}{p} \\ &= \frac{\partial R_0}{\partial p} \times \frac{p}{R_0} \end{aligned}$$

where  $R_0$  is explicitly defined in equation 3.11.

**Table 3:** Sensitivity Indices of the Basic Reproduction Number,  $R_0$

Parameters	Signs	Values
$\alpha_h$	+	0.52169
$\mu_h$	-	0.5
$\beta_c$	+	0.8
$\beta_h$	+	0.67590
$\delta_h$	-	0.40167
$\sigma_h$	-	0.26543
$\gamma_2$	-	0.40923
$\gamma_1$	-	0.15560
$\gamma_4$	-	0.10578
$u_1$	-	0.61478
$u_2$	-	0.71146

In table 3 above, we present the sensitivity index of the baseline parameters which affect the basic reproduction number directly as contained in the  $R_0$  expression in equation 3.11. The sensitivity indices are obtained using the Maple software with parameter values for these calculations contained in table 2. A positive sensitivity index suggests that an increase in the value of such parameter by some percentage will increase the value of  $R_0$ , and hence increase the spread of the disease, by a certain percentage and vice versa. For instance,

$\Gamma_{\beta_c}^{R_0} = 0.8$  suggests that an increase in the value of  $\beta_c$  by 10% will increase the value of  $R_0$  by 8% and vice versa.

#### IV. Discussion and Conclusions

In this section, we present the discussions of the results obtained in the numerical simulations of the Lassa fever control model and then the conclusions of the research.

##### 4.1 Numerical Simulation of the Model

We solve the control model's differential equations 2.1 to 2.7 numerically using the MATLAB ode45 method. We then present the solutions to the model's state variables in graphical form with the simulation done over a period of time = 365 days. The initial conditions for this numerical simulation are chosen theoretically as  $S_h(0) = 150$ ,  $C_h(0) = 40$ ,  $I_h(0) = 30$ ,  $T_h(0) = 25$ ,  $R_h(0) = 25$ ,  $S_v(0) = 60$ , and  $I_v(0) = 10$ .

##### 4.1.1 Susceptible Human Population

Figure 2 depicts the behavior of the Susceptible human population,  $S_h$ , over a period of 365 days. During the first 20 days. This population experiences a reduction in size, associated majorly to the progression of its members into the Carrier population by the contraction of the infection. After this short duration, a continuous increase in the population size is experienced due to the loss of immunity of the recovered population and also the progression of new members into this population as the population is not closed. Figure 2(a) shows the effect of the contracting rate of the Susceptible human population via contact with the Infected human population,  $\beta_h$ , on the member of  $S_h$ . It is observed that an increase in  $\beta_h$  results in a decrease in the Susceptible human population and a significantly large value of  $\beta_h$  results in a significantly small value of  $S_h$ . Similarly, figure 2(b) depicts the effect of the control of vaccination,  $u_2$ , on the Susceptible human population. It is observed that an increase in  $u_2$  results in a decrease in  $S_h$ . Hence, the application of the vaccination control over time results in a consistent decrease in the number of humans susceptible to the Lassa fever disease.

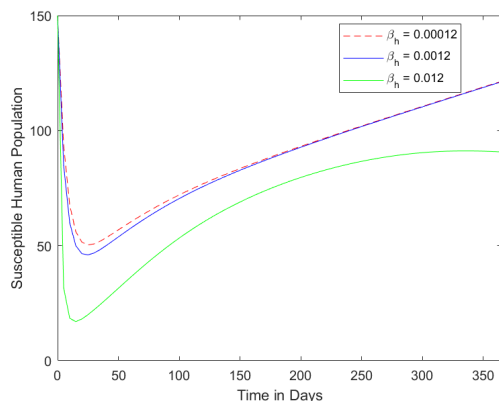


Figure 2(a): Variation of the values of parameter  $\beta_h$

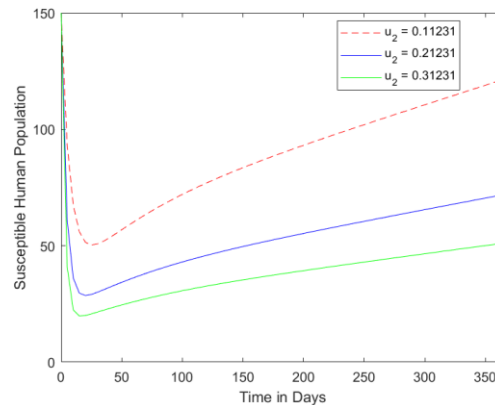


Figure 2(b): Variation of the values of parameter  $u_2$

**Figure 2:** Graphs of the Susceptible Human Population against Time

##### 4.1.2 Carrier Human Population

We present the behavior of the Carrier human population,  $C_h$ , in figure 3. During the first 100 days of the numerical simulation, this population is seen to experience a rapid and continuous reduction in its initial member size. This reduction is associated majorly to the use of the control of early diagnosis and treatment of its members at the rate  $u_1$ . After this rapid decrease has been experienced, the Carrier population is seen to decrease slowly from 2 members and gradually approaches 0 member for the remaining days of the simulation. An increase in the value of the three controls of early diagnosis and treatment of the Carrier population, vaccination of the Susceptible human population and the use of Rodenticide on the vector populations result in a decrease in the members of the Carrier human population as depicted in figures 3(a), 3(b) and 3(c) respectively. Similarly, an increase in the recovery rate of the Carrier population by natural immunity,  $\gamma_1$ , results in a decrease in the size of the population as its members proceed into the Recovered human population as shown in figure 3(d).

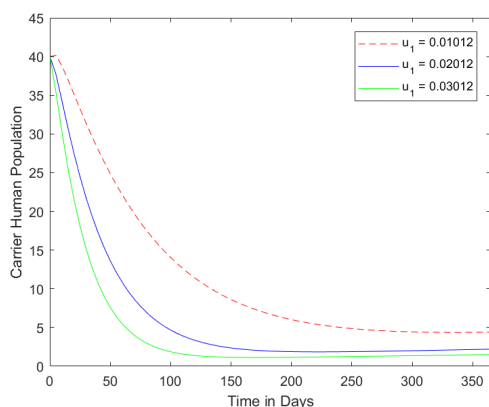


Figure 3(a): Variation of the values of parameter  $u_1$

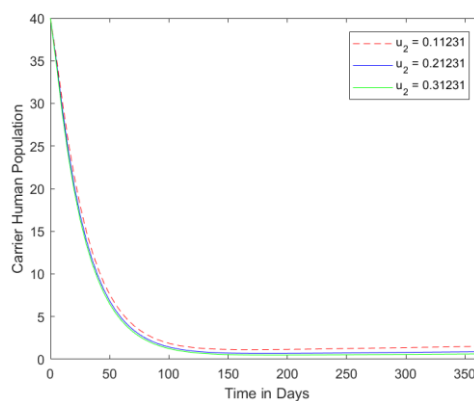


Figure 3(b): Variation of the values of parameter  $u_2$

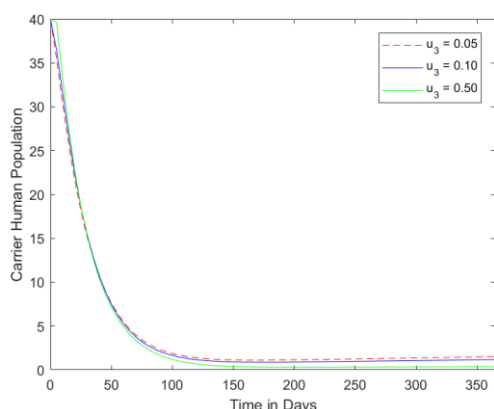


Figure 3(c): Variation of the values of parameter  $u_3$

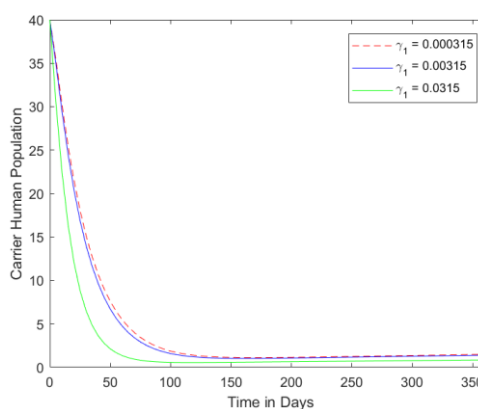


Figure 3(d): Variation of the values of parameter  $\gamma_1$

**Figure 3:** Graphs of the Carrier Human Population against Time

#### 4.1.3 Infected Human Population

Figure 4 depicts the behavior of the Infected human population,  $I_h$ , with respect to time. The infected human population experiences a rapid reduction in its member size at the beginning of the simulation until it converged at 0 members by the 100th day. This decrease is not only due to the treatment given to this population but also the early diagnosis and treatment of the Carrier human population which results in much lesser Carriers progressing to the fully blown infectious state. Figure 4(a) shows the effect of the control of vaccination,  $u_2$ , on the members of this population. It is observed that an increase in the value of  $u_2$  results in a decrease in the size of the Infected human population and the larger the value of  $u_2$ , the faster the infected population attain a 0 member. Similarly, the effect of changes in the rate of treatment of the Infected human population,  $\gamma_2$ , is shown in figure 4(b). It is observed that the higher the value of  $\gamma_2$ , the much faster the Infected human population approach 0 as its members progress into the Treated class. The incorporation of the controls  $u_1$ ,  $u_2$  and  $u_3$  into the Lassa fever pandemic results in the complete eradication of the Infected human population over a period of time.

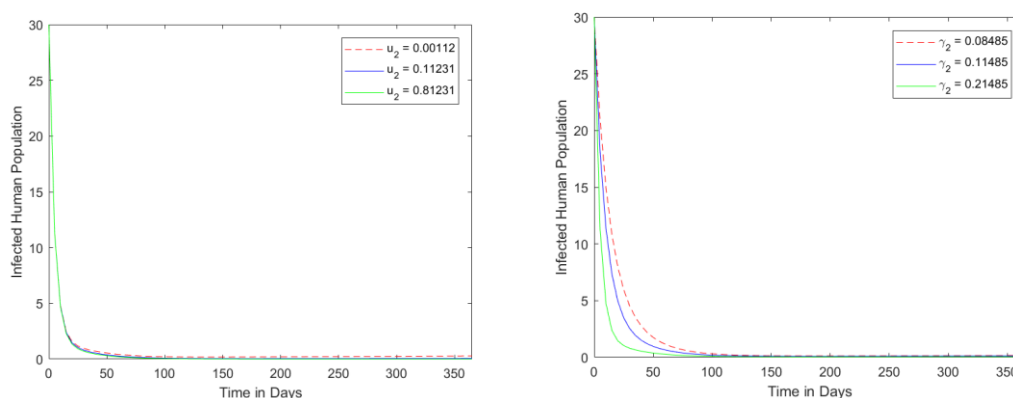
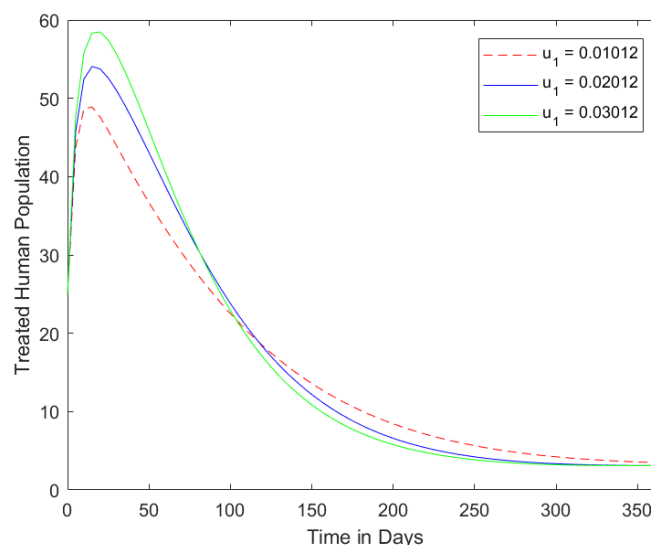


Figure 4(a): Variation of the values of parameter  $u_2$  Figure 4(b): Variation of the values of parameter  $\gamma_2$   
**Figure 4:** Graphs of the Infected Human Population against Time

#### 4.1.4 Treated Human Population

We present the behavior of the Treated human population,  $T_h$ , in figure 5. During the first 25 days of the numerical simulation, this population is seen to experience a rapid increase in its member size after which an inflection point is reached and then a decrease in the member size is experienced. The initial increase in the member size of this population is primarily associated with the progression of the Carrier and Infected human populations who are being treated into this population. As the members of this class become fully recovered, they proceed into the Recovered human population and hence a decrease in the size of the population after some time. It can be observed that an increase in the rate of early diagnosis and treatment of the Carrier human population,  $u_1$ , results in an initial increase in the member size of this population and then after some time a reduction is experienced as its members recover.



**Figure 5:** Graph of the Treated Human Population against Time varying Parameter  $u_1$

#### 4.1.5 Recovered Human Population

Figure 6 depicts the behavior of the Recovered human population,  $R_h$ , with respect to time. The Recovered human population experiences a continuous increase in its member size throughout the period of the numerical simulation. This increase is not only due to the introduction of vaccination which moves the Susceptible human population to the Recovered population but also due to the efficacy of the treatment being received by the Carrier and Infected human populations. It is observed that an increase in the treatment factor,  $\beta$ , results in an increase in the member of the Recovered human population. Similarly, since the Recovered human population never experience a decrease in its size at any point of the simulation, it can be inferred that even though there exists a loss of immunity for the recovered humans, this immunity loss is not significant enough to affect the efficiency of the treatment and controls being used in eradicating the disease.

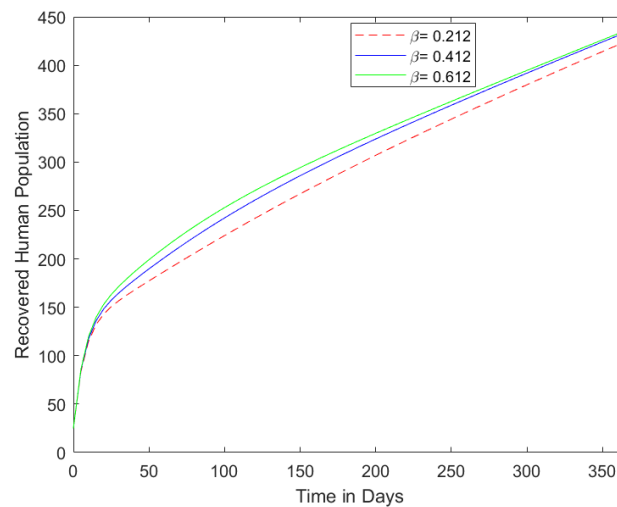


**Figure 6:** Graph of the Recovered Human Population against Time varying Parameter  $\beta$

#### 4.1.6 Susceptible Vector Population

Figure 7 represents the behavior of the Susceptible vector population,  $S_v$ , against time. The Susceptible vector population is seen to experience a continuous decrease in its member size during the first 50 days of the numerical simulation and then the population is maintained at a relatively low size afterwards. The initial reduction in the member size of this population is primarily associated with the use of the control of Rodenticide,  $u_3$ , which results in the death of its members. Since this population is not closed and more vectors could migrate from outside the population into it, it is observed that after about 50 days, an equilibrium state is attained between the number of vectors coming in and moving out of this population either to the Infected population or lost to death. Furthermore, an increase in the rate at which the Rodenticide control is administered results in an increase in the rate at which this population reduces in size.

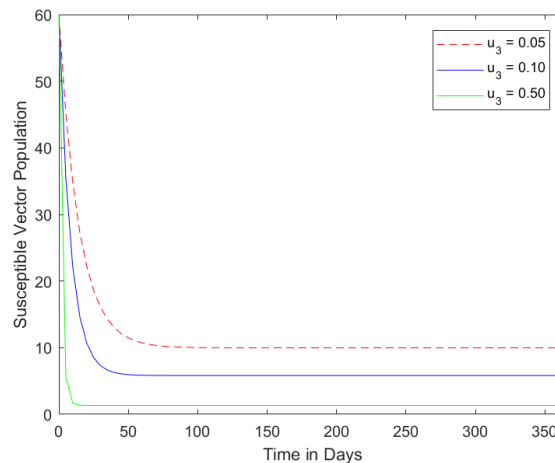


**Figure 7:** Graph of the Susceptible Vector Population against Time varying Parameter  $u_3$

#### 4.1.7 Infected Vector Population

Figure 8 depicts the behavior of the Infected vector population,  $I_v$ , against time. The Infected vector population experiences a continuous decrease in its member size during the first few and then the population is maintained at a relatively low size afterwards. It is observed that the higher the rate at which the control of Rodenticide is being administered, the faster the rate of reduction in the size of the population. In fact, if the control of Rodenticide is used at a significantly large rate, then the size of this population is seen to not only approach zero but also converge at zero before the 50th day of the simulation. Hence, this control is highly efficacious in preventing the spread of the LF disease among the vector hosts.

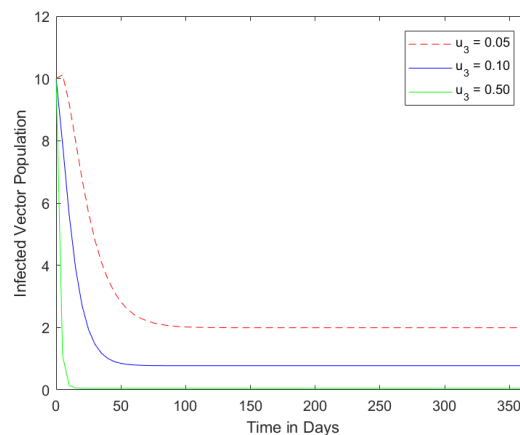


**Figure 8:** Graph of the Infected Vector Population against Time varying Parameter  $u_3$

#### 4.2 Conclusions

This research has brought into limelight the invaluable significance of the three controls of early diagnosis of the human infection before onset of noticeable symptoms resulting in the treatment of the human-carriers, vaccination of the susceptible humans and the use of Rodenticide on the vector populations as effective means of limiting the spread of Lassa fever disease within an endemic population. An increase in the value of these three controls, as shown in the numerical simulations results, yields a rapid and continuous decrease in the members of the carrier human, infected human and vector populations and eventually results in the eradication of the disease from an endemic population. Similarly, the recovered population experiences a continuous increase and no decrease in its size for the entire simulation and this suggests that these controls are very efficacious in controlling the disease.

The region within which the solution of the model's equations are contained, the model's invariant region, is positively invariant and hence the model is epidemiologically and mathematically well-posed. Hence, the implementation of the model into a LF endemic population will yield the desired results as demonstrated in this research.

The stability analyses results show that the basic reproduction number,  $R_0$ , obtained for the developed control model is significantly small and lesser than that obtained by Akinade et al. (2019) in which the analyzed model do not contain any control strategy. This implies that the incorporation of the controls  $u_1, u_2$  and  $u_3$  reduces the average number of secondary infections generated by a single infected individual during their entire infectious period. Hence, since the DFE is locally asymptotically stable, then the disease will not invade the population though it may persist for a short period of time, during which the controls are being implemented, due to its global instability.

The sensitivity analyses results show the sensitiveness of each model parameter to the transmission of the disease and it was obtained that the rate at which the susceptible human population contracts the infection via contact with a human-carrier,  $\beta_c$ , is the most sensitive parameter to the spread of the disease. This suggests that reducing this parameter value to a significantly small value will significantly reduce the value of  $R_0$  and result in a much lesser secondary infection.

It can be concluded that the application of the findings of this research into a Lassa fever disease endemic population is not only significant but pertinent to eradicating the disease from such an area.

#### 4.3 Recommendations

From the conclusions of this research work, it is highly recommended that early diagnosis of all suspected Lassa fever infections be carried out in order to determine those that are asymptotically infected. Also, diagnostic kits should be made readily available by the government agencies, health organizations and policy makers to all Lassa fever endemic areas and an infected individual, even while without symptoms, should be provided with resources to commence and maintain treatment.

Similarly, the government and health organizations are advised to make available effective vaccine(s) for the prevention of the disease just as it was recently made available for yellow fever in Nigeria and the result thereafter in terms of the control of the disease is priceless. Similarly, individuals living within the disease endemic areas are advised to continually make use of Rodenticide in their houses and environs, while ensuring that this Rodenticide do not come in contact with their household consumables, as this will help in preventing the invasion of the house/community by infected rodents.

#### **4.4 Areas for Further Research**

In order to obtain which combination of control will yield the most cost effective optimal result, cost effectiveness analyses of each control should be carried out. Similarly, the effect of the unprecedented climate crisis on the spread and control of Lassa fever disease should be examined.

#### **Acknowledgments**

I acknowledge the African Union for the rare opportunity afforded me to have my master's degree study in a high-class university of postgraduate study, the Pan African University Institute for Basic Sciences, Technology and Innovation (PAUSTI). Part of this paper is an extract from my master's research work at PAUSTI.

#### **References**

- [1]. Adewale, S., Olopade, I., Ajao, S., Adeniran, G., and Oyedemi, O. (2016). Mathematical analysis of lassa fever model with isolation. *Asian Journal of Natural & Applied Sciences*, 5(3), pp 47-57.
- [2]. Afolabi, A. and Sobowale, A. (2017). A mathematical model for the control of lassa fever. *Transaction of the Nigerian association of mathematical physics*, 5(September and November, 2017), pp 279-284.
- [3]. Akinade, M. O., Afolabi, A. S., and Kimathi, M. E. (2019). Mathematical modeling and stability analyses of lassa fever disease with the introduction of the carrier compartment. *Journal of Mathematical Theory and Modeling*, 9(6), pp 45-62.
- [4]. Akinpelu, F. O. and Akinwande, R. (2008). Mathematical model for lassa fever and sensitivity analysis. *Journal of Scientific and Engineering Research*, 5(6), pp 1-9.
- [5]. Bawa, M., Abdulrahman, S., Jimoh, O., and Adabara, N. (2013). Stability analysis of the Disease-free equilibrium state for lassa fever disease. *Journal of Science, Technology, Mathematics and Education (JOSTMED)*, 9(2), pp 115-123.
- [6]. Castillo-Chavez, C. and Song, B. (2004). Dynamical models of tuberculosis and their applications. *Mathematical biosciences and engineering*, 1(2), pp 361-404.
- [7]. CDC (2018). Act against aids, retrieved from <https://www.cdc.gov/actagainstaids/basics/transmission.html> on 01/09/2018 at 22:05gmt.
- [8]. Du-Toit, A. (2018). Lassa fever outbreak in nigeria, retrieved from <http://dx.doi.org/10.1038/nrmicro.2018.39> on 01/09/2018 at 12:15gmt. *Nature Reviews Microbiology*, 16(260).
- [9]. Eze, K., Salami, T., Eze, I., Pogoson, A., Omordia, N., and Ugochukwu, M. (2010). High lassa fever activity in northern part of edo state, nigeria: reanalysis of confirmatory test results. *African Journal of Health Sciences*, 17(3&4), pp 52-56.
- [10]. James, T. O. and Akinyemi, S. (2015). Stability analysis of lassa fever with quarantine and permanent immunity. *International Journal of Applied Science and Mathematical Theory*, 1(8), pp1-11.
- [11]. NCDC (2019). Nigeria centre for disease control situation report, retrieved from <http://www.ncdc.gov.ng/diseases/sitreps/> on 10/07/2019 at 09:20GMT.
- [12]. Obabiyi, O. and Onifade, A. A. (2017). Mathematical model for lassa fever transmission dynamics with variable human and reservoir population. *International Journal of Differential Equations and Applications*, 16(1), pp 67-91.
- [13]. Ogabi, C., Olusa, T., and Madufor, M. (2012). Controlling lassa fever transmission in northern part of edo state, nigeria using sir model. *New York Science Journal*, 5(12), pp 190-197.
- [14]. Omale, D. and Edibo, T. E. (2017). Mathematical models for lassa fever transmission with control strategies. *Computing, Information Systems, Development Informatics & Allied Research Journal*, 6(4), pp 25-31.
- [15]. Onuorah, M., Ojo, M., Usman, D., and Ademu, A. (2016a). Basic reproductive number for the spread and control of lassa fever. *International Journal of Mathematics Trends and Technology (IJMTT)*, 30, pp 1-7.
- [16]. Onuorah, M., Akinwande, N., Nasir, M., and Ojo, M. (2016b). Sensitivity analysis of lassa fever model. *European Centre for Research Training and Development, UK*, 4(1), pp 30-49.
- [17]. Van den Driessche, P. and Watmough, J. (2002). Reproduction numbers and sub-threshold endemic equilibria for compartmental models of disease transmission. *Mathematical bio-sciences*, 180(1-2), pp 29-48.
- [18]. WHO (2018). Infectious diseases, retrieved from <http://www.who.int/topics/infectious.diseases/en/> on 17/09/2018 at 13:20GMT.

#### **Appendix**

The following table contains some Lassa fever statistics in Nigeria for a period of 6 months (January to June, 2019) as provided by the NCDC (2019). The data contained in this table were used in obtaining the parameter values for some of the parameters contained in table 2.

**Table 4:** Table of Values for the Control Model's Parameter Value Calculation

Week No.	New Confirmed Cases	Total/Updated Suspected Cases	Total/Updated Positive Cases	Total/Updated Probable Cases	Total/Updated Negative Cases	Total Number Being Treated	New deaths Recorded
1	25	57	25	-	32	25	7
2	35	172	60	-	112	46	8
3	74	377	136	1	240	81	12
4	77	538	213	2	325	102	11
5	68	731	275	3	453	98	14
6	37	947	324	3	620	91	10
7	25	1139	355	3	781	88	6
8	23	1249	381	15	858	55	6
9	39	1374	420	15	939	69	8
10	52	1752	472	15	1265	68	11
11	23	1801	495	15	1277	63	4
12	15	1924	510	15	1511	32	5
13	16	2061	521	15	1525	30	2
14	11	2133	537	15	1581	21	1
15	3	2217	540	15	1662	13	0
16	6	2289	546	15	1728	13	1
17	8	2323	554	15	1754	13	1
18	11	2374	565	15	1794	11	4
19	4	2426	569	15	1842	8	0
20	6	2504	575	15	1914	5	1
21	3	2582	578	15	1989	6	0
22	3	2639	581	15	2043	5	1
23	6	2699	587	15	2097	4	1
24	4	2763	591	15	2157	3	1
25	10	2833	601	17	2215	12	3
26	2	2882	603	17	2262	8	1

Mary Oluwabunmi AKINADE.et.al. "Sensitivity And Stability Analyses Of A Lassa Fever Disease Model With Control Strategies." *IOSR Journal of Mathematics (IOSR-JM)*, 16(1), (2020): pp. 29-42.